Plasma Phys. Control. Fusion **42** (2000) L13–L22. Printed in the UK PII: S0741-3335(00)08209-9

LETTER TO THE EDITOR

Evidence for strange kinetics in Hasegawa–Mima turbulent transport

S V Annibaldi†, G Manfredi‡, R O Dendy§ and L O'C Drury†

† School of Cosmic Physics, Dublin Institute for Advanced Studies, 5 Merrion Square, Dublin 2, Republic of Ireland (Association Euratom/DCU)
‡ Laboratoire de Physique des Milieux Ionisés, Université Henri Poincaré, BP239, 54506 Vandoeuvre-les-Nancy, France
§ EURATOM/UKAEA Fusion Association, Culham Science Centre, Abingdon, Oxfordshire, OX14 3DB, UK

Received 28 September 1999, in final form 5 January 2000

Abstract. We have studied the transport of test particle ensembles moving in turbulent electrostatic fields governed by the Hasegawa–Mima (HM) equation. As a result of the interplay of the linear dispersive term and the nonlinear term in the HM equation, 'strange kinetics' emerge: the poloidal particle transport undergoes a qualitative transition from diffusive, through supradiffusive, to ballistic.

1. Introduction

There is increasing interest in the possibility that 'strange' (non-Gaussian) kinetics, including Lévy processes [1–3], may underly some aspects of energy and particle transport and confinement in magnetic fusion plasmas. It has long been realised that behaviour more complex than standard (Gaussian) diffusion can occur in Hamiltonian dynamics. In Gaussian diffusion, it is assumed that the motion can be described by a random walk dominated by short-step events, whose distribution has a finite variance. This, by the central limit theorem, ensures that the distribution of an ensemble of 'random walkers' tends (for large times) to a Gaussian, which acts as an attractor. By contrast, there are cases where the statistics are dominated by long-step events, such that the probability distribution has an infinite variance. In such cases, the distribution of the random walkers tends to an attractor which, instead of a Gaussian, is rather a Lévy distribution. This is described by a characteristic function (Fourier transform of the probability distribution) of the type $P(q) = K \exp(-c|q|^{\alpha})$, where $0 < \alpha < 2$ and K and c are constants. In real space, Lévy distributions display an algebraic tail $|x|^{-\alpha-1}$, implying that there is no characteristic size for the random walk steps [1, 4]. The only exception is the Gaussian, which corresponds to the value $\alpha = 2$, and whose moments are all finite. Numerical and experimental evidence for strange kinetics has been obtained in the past for ordinary fluids [5, 6]. Experiments with two-dimensional (2D) rotating fluids [6] are particularly relevant to our study, since it is well known that the Hasegawa–Mima (HM) equation (on which our results are based) is formally identical to the Charney equation for 2D rotating fluids [7]. In plasma confinement physics, there is emerging, albeit incomplete, evidence for an unexplained nexus that may encompass strange kinetics, Lévy processes, various forms of power law spectra, and self-organized criticality: see for example [8–14].

0741-3335/00/040013+10$30.00

Since anomalous transport in magnetic fusion plasmas is believed to be driven by underlying turbulent processes, it is worthwhile to investigate mathematical models to see whether evidence for supradiffusive (perhaps Lévy) transport can emerge naturally from first-principles models of plasma turbulence. For the case of magnetic turbulence in plasmas, which is significant for particle and energy transport in certain fusion contexts (for a recent review see [15]), it has already been shown that supradiffusion can arise. For example, in a seminal paper modelling the anomalous transport of cosmic ray electrons in magnetic turbulence in terms of a continuous time random walk, Ragot and Kirk [16] demonstrated mathematically the emergence of supradiffusion, and suggested that observations of diffuse radio emission from the Coma cluster can best be interpreted in terms of supradiffusive transport of cosmic ray electrons. It is therefore timely to investigate whether supradiffusion can also arise in electrostatic turbulence, which is believed to play a dominant role in most aspects of anomalous transport in magnetic fusion plasmas. Accordingly, in the present paper we investigate the implications for particle transport of a simple but widely studied paradigmatic model for strong 2D electrostatic turbulence in magnetized plasmas, the HM equation [17].

The physics of the HM equation is dominated by the $\boldsymbol{E} \times \boldsymbol{B}$ drift and involves low-frequency (compared to the ion cyclotron frequency ω_{ci}) waves driven unstable by the presence of a density or temperature gradient. In order to study the basic features of particle transport, we use the HM equation to provide a nonlinear model for drift turbulence in real space, whose output is the time-dependent electrostatic potential. This potential then acts as an input for the equations of motion of ensembles of test particles, whose orbits we follow and whose statistical properties we then infer. We have previously investigated radial particle transport in this way [18, 19], and found that nonlinear coupling significantly reduces the level of transport compared to the linear regime: this reduction was mainly ascribed to the formation of radial gradients in the velocity field. Now we turn to the poloidal component, and show that the HM model yields evidence for supradiffusive poloidal particle transport.

A similar problem was studied by Benkadda *et al* [20]. The main difference is that their electrostatic potential is made of a small number of interacting waves, whereas we focus our attention on broad-band turbulence (the reader should compare figure 3 of [20] with figures 3 and 4 of [19]). In addition, they do not distinguish explicitly between poloidal and radial dispersion. The amplitude of the waves is described by Benkadda *et al* in terms of a small set of differential equations, similar to the Lorenz model in fluid dynamics, and the nature of the resultant transport (normal or subdiffusive) is governed [20] by the presence of strange attractors.

The HM equation [17] is a relatively simple 2D model for the turbulent electrostatic field in the (x, y) plane perpendicular to the magnetic field ($\boldsymbol{B} \equiv B\hat{\boldsymbol{z}}$), and has many wider physical applications [21]. The model assumes cold ions: $T_{\mathrm{i}} \ll T_{\mathrm{e}}$ ($T_{\mathrm{i(e)}}$ being the ion (electron) temperature), with negligible inertia parallel to $\boldsymbol{B}$. The quasineutrality condition $n_{\mathrm{i}} \simeq n_{\mathrm{e}}$ is satisfied, where $n_{\mathrm{i(e)}}$ is the ion (electron) density; the electrons are assumed to have an immediate adiabatic response, with Boltzmann distribution; their background density depends only on y, equivalent to the radial direction in a tokamak, $n_0 \equiv n_0(y)$. The HM equation is then written [17–19]:

$$\frac{\partial}{\partial t}(\phi - \nabla^2\phi) - \gamma\{\phi, \nabla^2\phi\} - \beta\frac{\partial\phi}{\partial x} = 0 \tag{1}$$

where x and y are normalized to the ion thermal Larmor radius $\rho_s = c_s/\omega_{\mathrm{ci}}$, where $c_s = \sqrt{T_{\mathrm{e}}/m_{\mathrm{i}}}$ is the speed of sound and m_{i} the ion mass; the time t is normalized to L/c_s, where L is a characteristic length of the system; ϕ is the electrostatic potential normalized to $(T_{\mathrm{e}}/e)(\rho_s/L)$; $\{A, B\} = \partial_x A\partial_y B - \partial_y A\partial_x B$ is the Poisson bracket; and

$$\beta = \mid \partial_y \ln[n_0(y)] \mid \tag{2}$$

is a parameter measuring the anisotropy of the background density gradient. The coefficient γ has been introduced as a useful switch in order to vary the relative magnitude of the linear and nonlinear terms, and particularly for comparison with the purely linear case, for which $\gamma = 0$. The linear limit of (1) is equivalent to the evolution of a collection of independent drift waves, each obeying the dimensionless dispersion relation

$$\omega_k = -\frac{\beta k_x}{1 + k^2}. \tag{3}$$

We have implemented [18, 19] equation (1) in a computational box of area $L_x \times L_y = 20 \times 20$, which is finite in the y-direction and periodic in the direction of propagation of drift waves, x, equivalent to the poloidal direction in a tokamak. To the right-hand side of (1) a dissipation term D has been added, both for high and low wavenumbers, for reasons of numerical stability, and also a forcing term S in order to reach a quasi-stationary state [18, 19]. These terms have the following form in Fourier space:

$$D_k = -(\nu k^4 + \alpha)(1 + k^2)\phi_k \qquad S_k = A_k \delta(\boldsymbol{k} - \boldsymbol{k}_f) \tag{4}$$

where ν and α are dissipation coefficients respectively at high and low wavenumbers; A_k and $\boldsymbol{k}_f$ are the amplitude and the wavenumber of the forcing (note that this is localized at high wavenumbers, $k_f \gg 1$). Equation (1) is solved numerically by means of a hybrid spline-spectral method coupled to a leap-frog integrator in time. Typically a mesh 512×512 is used.

By varying the magnitude of the coefficients β and γ in (1), one can control the relative importance of the nonlinear terms (which are isotropic) compared to the linear terms (anisotropic). The model is thus well suited to study the influence of anisotropy (a linear dispersive effect) on the poloidal transport of test particles. Even for moderate values of β, the electrostatic potential develops an anisotropic spectrum, shallower in k_y and steeper in k_x [22]. This is a signature of the presence of 'zonal flows', or potential structures elongated in the direction of propagation of drift waves (x), which have already been shown to have an impact on particle transport in the direction of the density gradient (y) [18, 19]. The HM equation can also support drifting nonlinear vortex structures. Such structures can trap particles for relatively long times, and therefore affect their diffusion rate. This effect has recently been studied by Naulin *et al* [23], who use a model similar to ours (the Hasegawa–Wakatani equations), but with different boundary conditions, periodic in both directions. It appears that with such boundary conditions the effect of zonal flows is reduced. Particles are trapped within the vortices for some time, but ultimately they become untrapped, so that the computed diffusion in [23] is approximately normal for both the radial and the poloidal directions.

2. Particle transport

In order to analyse the transport of test particles moving in the HM field, we create an ensemble of 3000 particles, whose motion is given by the $\boldsymbol{E} \times \boldsymbol{B}$ drift,

$$\frac{\mathrm{d}\boldsymbol{r}}{\mathrm{d}t} = \boldsymbol{B} \times \frac{\nabla\phi}{B^2}. \tag{5}$$

Here ϕ is the electrostatic potential resulting from the numerical solution of the HM equation, and we neglect the polarization drift. The equations of motion are Hamiltonian in form, with the real space (x, y) coinciding with the phase space and $H(x, y, t) = \phi(x, y, t)/B$. The test particles are non-interacting and without inertia, so that we consider only their guiding centre motion and not Larmor radius effects (but compare [18, 19]). They are initially randomly

distributed within a narrow vertical band. Recall that for normal diffusion (a classical random walk), the mean squared displacement

$$\langle \Delta x^2 \rangle = \frac{\sum_{i=1}^{N} (x_i - \langle x \rangle)^2}{N} \tag{6}$$

is proportional to time: $\langle \Delta x^2 \rangle \sim t$. If transport is anomalous ('strange kinetics' [1–3]), this becomes $\langle \Delta x^2 \rangle \sim t^{\mu}$: for $0 < \mu < 1$, we have sub-diffusion; for $1 < \mu < 2$, supradiffusion; and for $\mu = 2$, ballistic motion—particles move with constant velocity. The main purpose of the present paper is to evaluate the exponent μ for poloidal transport in turbulence governed by different regimes of the HM equation. We shall see that, for several such regimes, μ can be larger than unity—a clear signature of supradiffusive motion.

The equations of motion, equation (5), are solved numerically by means of a second-order leap-frog scheme, which displays little numerical diffusion. The $\boldsymbol{E} \times \boldsymbol{B}$ velocity field at the particle locations is computed by linear interpolation. The overall numerical scheme has been tested by taking a 'frozen' velocity field: in this case, the particles should simply rotate inside the vortices on closed orbits, with no diffusion. The scheme has correctly reproduced this behaviour, within good approximation, over a large number of rotations.

We performed two sets of computer experiments. First, holding γ fixed, we ran a series of simulations for different values of β, including the isotropic case $\beta = 0$. These simulations are carried out in a driven–damped regime, in order to achieve a quasi-stationary turbulent state. In a second series of simulations β is kept fixed, and several runs are performed for different values of γ, starting from the linear case, $\gamma = 0$. Since the reference case is now linear (therefore there is no mixing between wavenumbers), these runs are carried out in a slowly decaying regime (no forcing, small dissipation). The interest of these two approaches is that they are somewhat complementary: in the first set of runs, we start from a purely nonlinear case, and slowly add anisotropic wave propagation; in the second, we begin with a purely linear regime, and slowly add nonlinear effects. For both sets of runs, we study the transport of test particles in the periodic (poloidal) direction x, i.e. the direction of propagation of drift waves. The transport in the finite (radial) direction has already been studied in [18, 19], where the main result was that the combination of linear and nonlinear terms suppresses the radial diffusion.

2.1. Quasi-stationary turbulence

To analyse the effect of anisotropy on the poloidal transport of particles, we ran the HM test particle code for a range of values of β. The forcing and dissipation parameters defined in (4) are the following: $\nu = 6 \times 10^{-7}$, $\alpha = 1 \times 10^{-4}$, $A_k = 4$ and $\boldsymbol{k}_f \simeq (40, 40)$. All simulations are run for times much longer than the eddy turnover timescale of the turbulence [22]

$$\tau_E = \gamma^{-1} \left(\frac{1}{L_x L_y} \int_{L_x} \int_{L_y} |\nabla^2 \phi|^2 \, \mathrm{d}\boldsymbol{r} \right)^{-1/2} \tag{7}$$

which is of order $\tau_E \simeq 10$ for all the cases studied in this section.

When $\beta = 0$, i.e. the background density is isotropic, the diffusion appears normal. In figure 1 we plot the position of the diffused particles at a later time ($t \gg \tau_E$), when the initial conditions have been 'forgotten'. Figure 1(*a*) shows that, when $\beta = 0$, the particles approximately follow the underlying vortex structure, while occasionally jumping from one vortex to the next, which yields normal diffusion. When β is increased, the vortices start to move and mix, due to the (dispersive) drift motion introduced by the term $\beta \partial_x \phi$ in the HM equation. The distribution of particles is shown in figures 1(*b*) and (*c*) for $\beta = 0.05$ and $\beta = 0.25$, respectively.

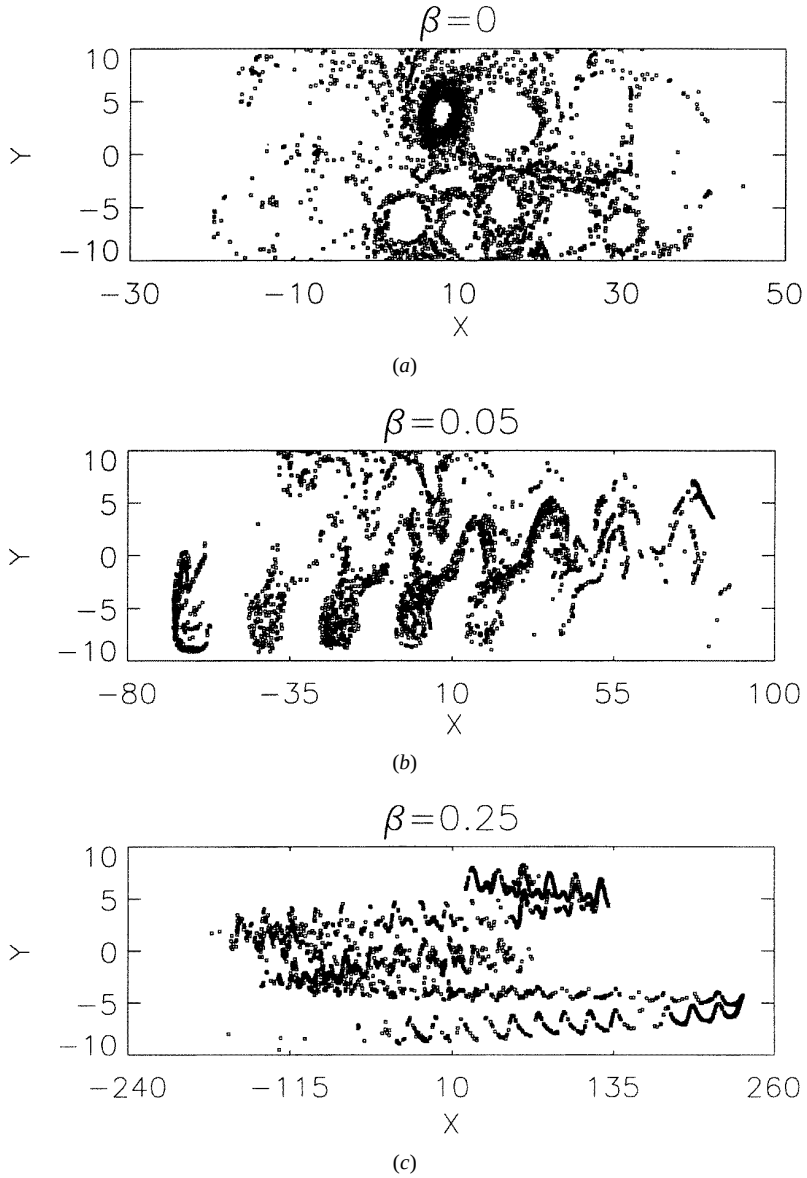

Figure 1. Position of the diffused particles in the forced case, with $\gamma = 1$ and box dimensions $L_x \times L_y = 20 \times 20$: (*a*) $\beta = 0$, the particles roughly show the underlying vortex structure; (*b*) $\beta = 0.05$; and (*c*) $\beta = 0.25$.

The mean square displacement of the particles $\langle \Delta x^2 \rangle$ is shown in figure 2, divided by t^μ, with the value of μ chosen to give the best fit to a constant curve at large times. As anticipated above, for $\beta = 0$ the diffusion appears normal, $\mu \simeq 1$. When β is increased the particles undergo supradiffusion, yielding $\mu \simeq 1.7$ for $\beta = 0.05$. If β is increased up to 0.25 or beyond, the motion of test particles becomes ballistic, with $\mu = 2$.

For a normal random walk, the particle distribution should be Gaussian at large times. A measure of the proximity of a distribution to a Gaussian is given by its kurtosis (peakedness),

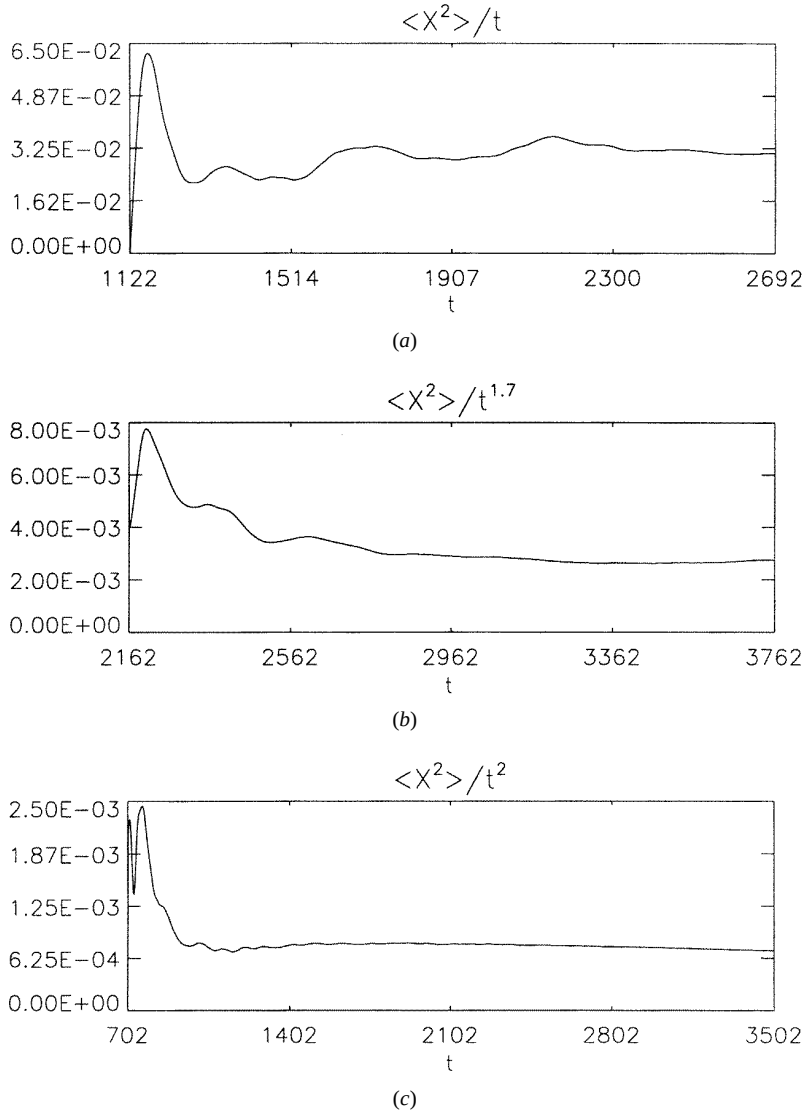

Figure 2. Plots of $\langle x^2\rangle/t^{\mu}$ against time, with μ chosen to give the best fit to a constant curve. Forced case, $\gamma = 1$ and box dimensions $L_x \times L_y = 20 \times 20$: (*a*) $\beta = 0$, $\mu \simeq 1$, normal diffusion; (*b*) $\beta = 0.05$, $\mu \simeq 1.7$, supradiffusion; and (*c*) $\beta = 0.25$, $\mu \simeq 2$, ballistic motion.

which we define here as $K = \langle \Delta x^4\rangle/3\langle \Delta x^2\rangle^2$. A Gaussian distribution has $K = 1$, whereas a more peaked distribution has $K > 1$, and a flatter-than-Gaussian distribution has $K < 1$; for example, the kurtosis of a rectangular distribution is 0.6. We have plotted the poloidal distribution of test particles for the cases studied above. It appears that the distribution is rather close to a Gaussian for $\beta = 0$, figure 3(*a*), whereas it is significantly flatter for $\beta = 0.25$, figure 3(*c*); the case $\beta = 0.05$, figure 3(*b*), is a transition between the other two. This is reflected in the measured value of the kurtosis, which is $K \simeq 1.2$ for $\beta = 0$. The small difference may be due to the large vortex present around $x = 0$, which causes the distribution to be slightly more peaked than a Gaussian (figure 3(*a*)). For $\beta = 0.25$, we find $K \simeq 0.73$, which is rather close to $K = 0.6$, the kurtosis of a rectangular distribution. Indeed, for a population of particles

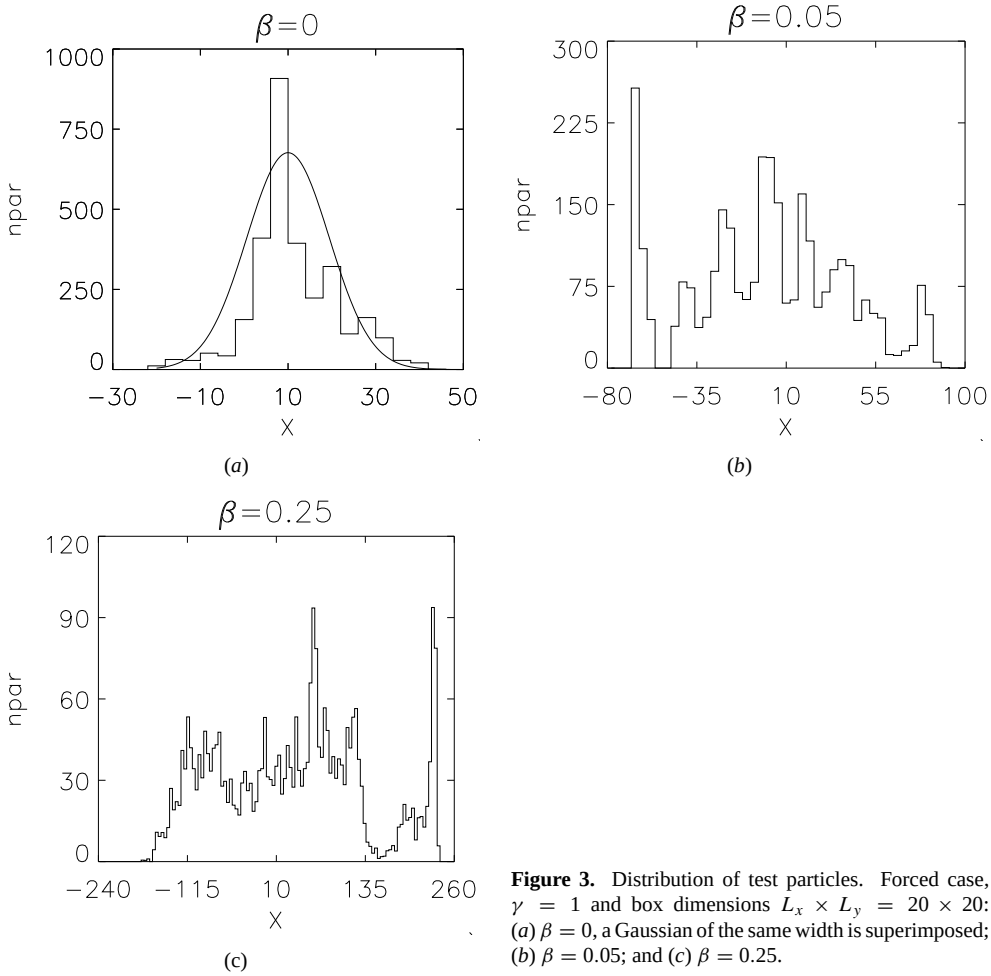

Figure 3. Distribution of test particles. Forced case, $\gamma = 1$ and box dimensions $L_x \times L_y = 20 \times 20$: (*a*) $\beta = 0$, a Gaussian of the same width is superimposed; (*b*) $\beta = 0.05$; and (*c*) $\beta = 0.25$.

starting from a central band and all having ballistic motion, the resulting distribution should be rectangular. The peak visible on figure 3(*c*) (and, to a lesser extent, also figure 3(*b*)) seems to be due to a group of particles that move coherently in the velocity field. Such a peak is also present in the large β runs presented in the next section. This could suggest that, in the presence of a significant β-effect (i.e. a steep equilibrium density gradient), the separation of neighbouring trajectories is slower than exponential.

2.2. Decaying turbulence

We now turn to the study of poloidal transport in a slowly decaying turbulent field. Note that the decay time is much longer than the typical diffusion time for the test particles, so that, for practical purposes, the turbulence can still be regarded as quasi-stationary. Keeping β fixed and equal to 0.1, we select increasingly large values for the parameter γ in the HM equation, thus raising the relative strength of the nonlinear effects. The reference run is now purely linear ($\gamma = 0$), and the relevant time scale τ_L is therefore given by the inverse of a typical value of the linear frequency (equation (3)). Since the k-spectrum is dominated by small and intermediate wavenumbers $k < 5$, a typical time scale is $\tau_L \simeq 20$. All simulations are run for times much longer than τ_L. The forcing and dissipation parameters in (4) are the following: $A_k = \alpha = 0$

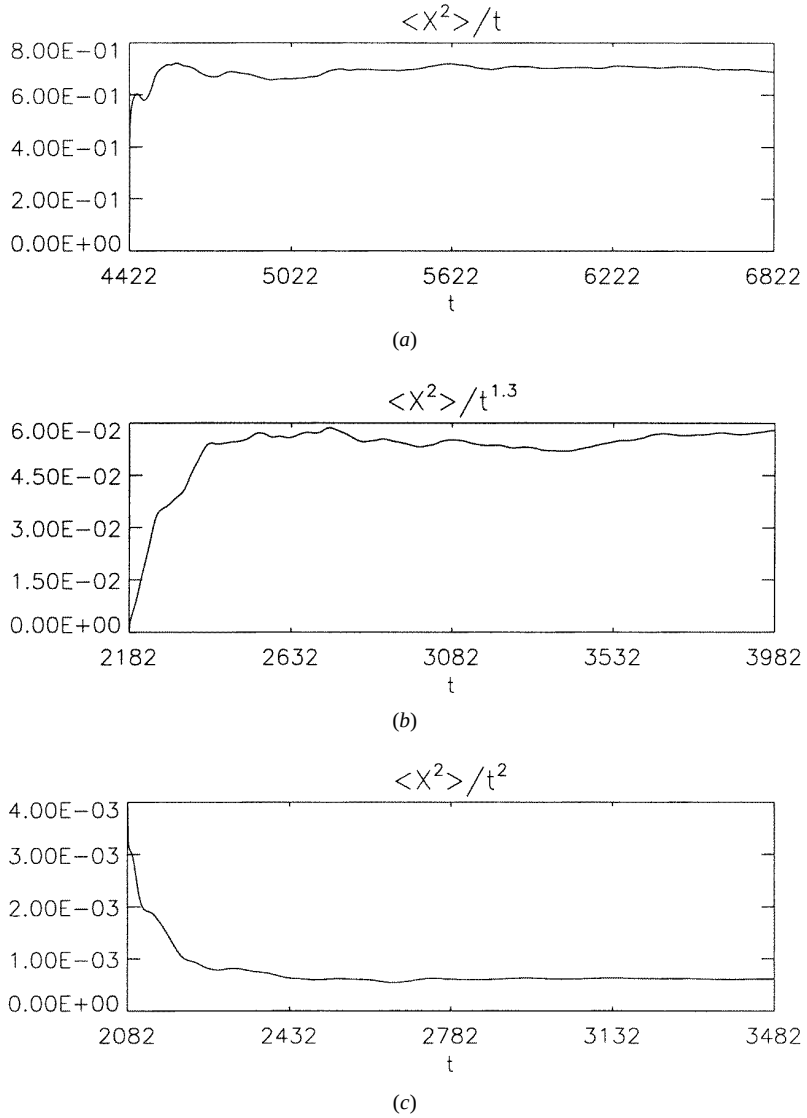

Figure 4. Plots of $\langle x^2 \rangle / t^{\mu}$ against time, with μ chosen to give the best fit to a constant curve. Decaying case, with $\beta = 0.1$ and box dimensions $L_x \times L_y = 20 \times 20$: (*a*) $\gamma = 0$, $\mu \simeq 1$, approximately normal diffusion; (*b*) $\gamma = 0.1$, $\mu \simeq 1.3$, supradiffusion; and (*c*) $\gamma = 0.5$, $\mu \simeq 2$, ballistic motion.

(no forcing and no large scale dissipation) and $\nu = 1 \times 10^{-7}$. The initial electrostatic potential chosen for this set of runs has a broad isotropic spectrum, roughly decaying as k^{-3}.

We ran the code for three different cases. When $\gamma = 0$ the HM equation is purely linear, and the particles evolve in a field which is made of a collection of independent drift waves. In this case the diffusion is approximately normal, figure 4(*a*), as was observed in previous simulations [24]. However, even for moderate values of γ, supradiffusion is observed, figures 4(*b*) and 4(*c*). The exponent μ is measured to be roughly 1.3 for $\gamma = 0.1$, while for $\gamma = 0.5$ or larger, we again observe ballistic motion ($\mu = 2$).

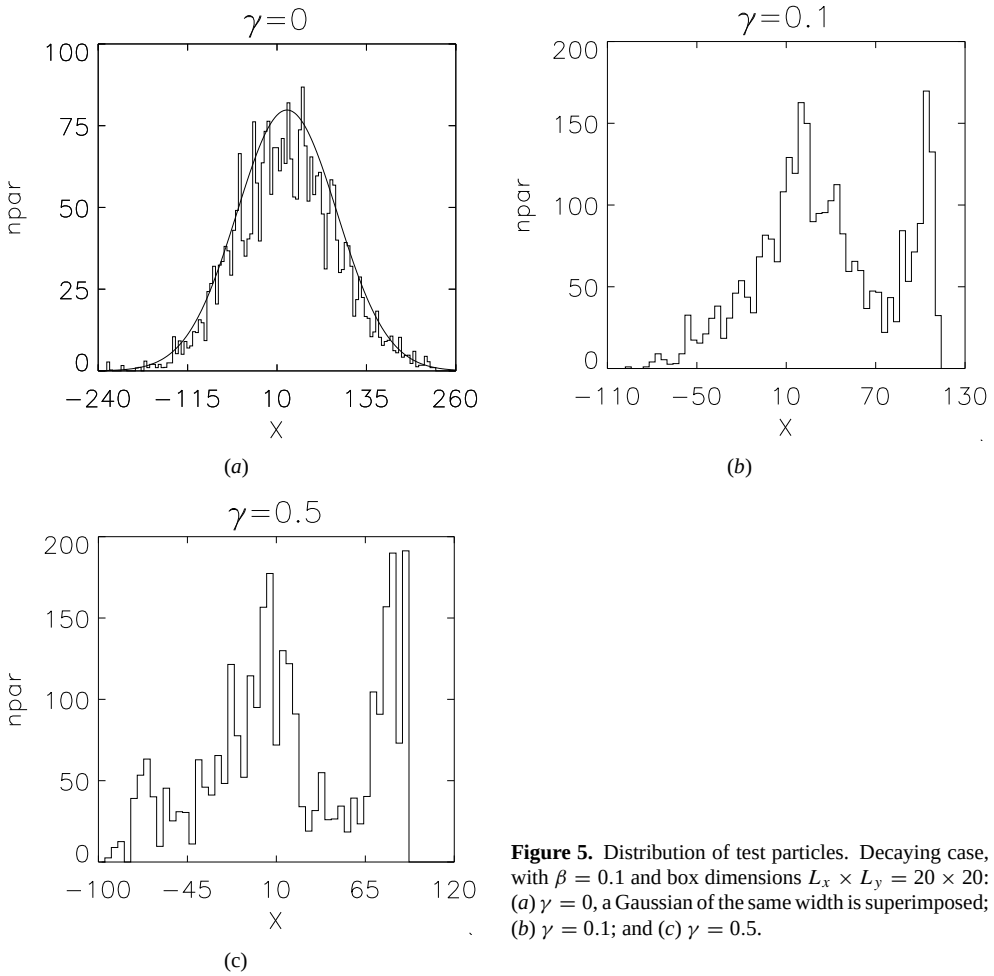

Figure 5. Distribution of test particles. Decaying case, with $\beta = 0.1$ and box dimensions $L_x \times L_y = 20 \times 20$: (*a*) $\gamma = 0$, a Gaussian of the same width is superimposed; (*b*) $\gamma = 0.1$; and (*c*) $\gamma = 0.5$.

The particle distributions display similar trends to those observed in the first set of simulations. Figure 5(*a*) shows the poloidal distribution of particles for $\gamma = 0$, which appears to be close to a Gaussian. Its kurtosis also approaches unity for sufficiently long times ($K \simeq 1$). For $\gamma = 0.1$, however, the particle distribution is not Gaussian (figure 5(*b*)) and $K \simeq 0.77$. For $\gamma = 0.5$ the particle distribution is even flatter (figure 5(*c*)), and its kurtosis is $K \simeq 0.68$.

3. Conclusions

We have studied the transport of test particles in turbulent HM fields along the (poloidal) direction of propagation of drift waves. Two sets of simulations have been performed, for which the reference run is either a purely nonlinear or a purely linear case, and we change the balance between the linear and nonlinear effects by varying appropriate control parameters. This enables us to study poloidal particle transport in purely linear, purely nonlinear, and intermediate regimes. We find that, in the purely linear and purely nonlinear cases, the diffusion is normal, i.e. $\langle \Delta x^2 \rangle \sim t^{\mu}$, with $\mu \simeq 1$. However, when both linear and nonlinear terms are simultaneously present, we find a regime of enhanced diffusion (supradiffusion), leading to an exponent $\mu > 1$. Finally, when both terms are of comparable magnitude, the transport is ballistic ($\mu = 2$). It therefore appears that supradiffusion in the poloidal direction results from

the combined effects of the nonlinearity and the linear dispersive term in the HM equation. However, we have observed that supradiffusive or even ballistic transport occurs when the effect of the linear wavelike term (the β term) is still quite low. The potential fields of the three cases treated in both section 2.1 (driven–damped turbulence) and section 2.2 (decaying turbulence) do not differ much from each other. In particular, the third case of both sections does not appear to be dominated by zonal flows—although some differences are visible in the wavenumber spectra, indicating that some zonal flows are indeed present. Therefore, our study suggests that even a low level of linear wave effects can significantly affect particle transport in the direction parallel to wave propagation (poloidal direction). Particle transport in the perpendicular (radial) direction has already been studied in [18, 19], where the main result is that the combination of linear and nonlinear effects strongly reduces diffusion. We conclude from combining the results of the present study with those of [18, 19] that, at least for the model considered here, the simultaneous presence of nonlinearity and a background density gradient leads to enhanced 'strange kinetic' transport of particles in the poloidal direction, but reduces particle transport in the radial direction. The observed 'strange kinetics' poloidal transport might be associated with a non-Gaussian probability distribution of the step sizes in the underlying random walk. Such step sizes may appear as long jumps in the particle trajectories, leading to a Lévy-type distribution for the test particles. The relation between the distribution of the step sizes and the observed supradiffusive exponents μ will be the subject of future work.

This work was supported in part by the UK Department of Trade and Industry and Euratom. SVA is grateful for the support of a Marie Curie predoctoral fellowship awarded by the Commission of the European Communities (Contract no 5004-CT97-5005).

References

[1] Shlesinger M F, Zaslavsky G M and Klafter J 1993 *Nature* **363** 31
[2] Zaslavsky G M, Stevens D and Weitzner H 1993 *Phys. Rev.* E **48** 1683
[3] Tsallis C, Levy S V F, Souza A M C and Maynard R 1995 *Phys. Rev. Lett.* **75** 3589
[4] Klafter J, Shlesinger M F and Zumofen G 1996 *Phys. Today* vol 49 February, 33
[5] Provenzale A 1999 *Ann. Rev. Fluid Mech.* **31** 55
[6] Solomon T, Weeks E and Swinney H 1993 *Phys. Rev. Lett.* **71** 3975
[7] Horton W and Hasegawa A 1994 *Chaos* **4** 227
[8] Carreras B A *et al* 1999 *Phys. Plasmas* **6** 1885
[9] Newman D E, Carreras B A, Diamond P H and Hahm T S 1996 *Phys. Plasmas* **3** 1858
[10] Carreras B A, Newman D, Lynch V E and Diamond P H 1996 *Plasma Phys. Rep.* **22** 740
[11] Dendy R O and Helander P 1997 *Plasma Phys. Control. Fusion* **39** 1947
[12] Chapman S C, Watkins N W, Dendy R O, Helander P and Rowlands G 1998 *Geophys. Res. Lett.* **25** 2397
[13] Watkins N W, Chapman S C, Dendy R O and Rowlands G 1999 *Geophys. Res. Lett.* **26** 2617
[14] Dendy R O, Helander P and Tagger M 1998 *Astron. Astrophys.* **337** 962
[15] Bickerton R J 1997 *Plasma Phys. Control. Fusion* **39** 339
[16] Ragot B and Kirk J G 1997 *Astron. Astrophys.* **327** 432
[17] Hasegawa A and Mima K 1977 *Phys. Fluids* **21** 87
[18] Manfredi G and Dendy R O 1996 *Phys. Rev. Lett.* **76** 4360
[19] Manfredi G and Dendy R O 1997 *Phys. Plasmas* **4** 628
[20] Benkadda S, Gabbai P and Zaslavsky G M 1997 *Phys. Plasmas* **4** 2864
[21] Hasegawa A 1985 *Adv. Phys.* **34** 1
[22] Manfredi G 1999 *J. Plasma Phys.* **61** 601
[23] Naulin V, Nielsen A H and Rasmussen J J 1999 *Phys. Plasmas* **6** 4575
[24] Pettini M, Vulpiani A, Misguich J H, De Leener M, Orban J and Balescu R 1988 *Phys. Rev.* A **38** 344